European Journal of Taxonomy 310: 1–32
https://doi.org/10.5852/ejt.2017.310

ISSN 2118-9773
www.europeanjournaloftaxonomy.eu
2017 · Van Ginneken M. *et al.*

Research article

urn:lsid:zoobank.org:pub:E07A58BA-7D3B-4231-9C77-97A031128E62

Morphometry and DNA barcoding reveal cryptic diversity in the genus *Enteromius* (Cypriniformes: Cyprinidae) from the Congo basin, Africa

Marjolein VAN GINNEKEN [1,†], Eva DECRU [2,*,†], Erik VERHEYEN [3] & Jos SNOEKS [4]

[1] Department of Biology, Systemic Physiological and Ecotoxicological Research, University of Antwerp, Groenenborgerlaan 171, 2020 Antwerpen, Belgium.
[2,4] Royal Museum for Central Africa, Section Vertebrates, Ichthyology, Leuvensesteenweg 13, 3080 Tervuren, Belgium.
[2,4] Department of Biology, Laboratory of Biodiversity and Evolutionary Genomics, KU Leuven, Charles Deberiotstraat 32, 3000 Leuven, Belgium.
[3] Royal Belgian Institute of Natural Sciences, OD Taxonomy and Phylogeny, Vautierstraat 29, 1000 Brussels, Belgium; Department of Biology, Evolutionary Ecology Group, University of Antwerpen, Campus Drie Eiken, building D, room D.150 Universiteitsplein 1, 2610 Antwerpen, Belgium.
† Equally contributing authors

* Corresponding author: eva.decru@africamuseum.be
[1] Email: marjolein.vanginneken@uantwerpen.be
[3] Email: everheyen@naturalsciences.be
[4] Email: jos.snoeks@africamuseum.be

[1] urn:lsid:zoobank.org:author:FDADB435-8B18-49C9-B803-F925ABF21A22
[2] urn:lsid:zoobank.org:author:1AEB7EED-C939-4702-8590-B3FCA7076324
[3] urn:lsid:zoobank.org:author:86B40463-E3D9-4147-9ED3-D7302E0D64B6
[4] urn:lsid:zoobank.org:author:13A8AB26-FF46-437C-9806-D49E11C5E15D

Abstract. One of the main challenges to adequately conserve the African fish fauna is to improve our so far unsatisfactory taxonomic knowledge of important portions of the ichthyofauna. In the present study, we attempted to unravel the taxonomic diversity of some species of *Enteromius* Cope, 1867, a problematic African fish genus, recently collected in the north-eastern part of the Congo basin. We used an integrative approach, combining DNA barcodes and morphological analyses. For one of the species complexes found, the *E. miolepis/eutaenia* species complex, we evaluated taxonomic diversity over a larger geographic scale within the Congo drainage system. Although initial literature-based species identifications allowed us to assign all examined specimens to four tentative species, DNA barcodes indicated the presence of 23 distinct mitochondrial lineages. The majority of these lineages appeared endemic to particular rivers, and in most rivers multiple lineages occur in sympatry. Subsequent exploratory morphometric analyses indicated that almost all these lineages are morphologically distinguishable and that they may therefore represent undescribed species. As only a part of the Congo basin and a subset of the species diversity within *Enteromius* were examined, it appears that the species richness of *Enteromius* in the Congo basin is severely underestimated.

Keywords. '*Barbus*', COI, integrative taxonomy, species richness.

Van Ginneken M., Decru E., Verheyen E. & Snoeks J. 2017. Morphometry and DNA barcoding reveal cryptic diversity in the genus *Enteromius* (Cypriniformes: Cyprinidae) from the Congo basin, Africa. *European Journal of Taxonomy* 310: 1–32. https://doi.org/10.5852/ejt.2017.310

Introduction

With some 3060 species in about 375 genera already described (Froese & Pauly 2017), Cyprinidae is the largest family of freshwater fishes in the world. Within this family, the former genus *Barbus* sensu lato (s.l.) Cuvier & Cloquet, 1816, was a very extensive paraphyletic aggregation of over 800 species occurring in Europe, Africa and Asia. Based on ploidy level, *Barbus* s.l. has been divided into three groups: diploids (2n = 48 or 50), tetraploids (2n = 100) and hexaploids (2n = 148–150) (Agnèse *et al.* 1990; Oellerman & Skelton 1990; Rab *et al.* 1995; Berrebi & Valiushok 1998). The phylogeny of some of these groups has been examined (e.g., Agnèse *et al.* 1990; Tsigenopoulos *et al.* 2010), and a number of studies suggested to split *Barbus* s.l. into several genera at least based on the level of ploidy (Berrebi *et al.* 1996). Due to their uncertain taxonomic position, the African small-sized diploid species were, until recently, referred to as '*Barbus*' (between quotation marks) as proposed by Berrebi *et al.* (1996). A recent study explored the classification of the subfamily Cyprininae that includes *Barbus* s.l., using mitochondrial and nuclear genes (Yang *et al.* 2015). The results of this study supported a close relationship within the diploid species between the Asian *Puntius* Hamilton, 1822 species and the African small '*Barbus*'. As such, they confirmed earlier results based on karyology (Golbutsov & Krysanov 1993; Rab *et al.* 1995). Yang *et al.* (2015) proposed the revalidation of the genus *Enteromius* Cope, 1867 to accommodate all African diploid '*Barbus*' species, as it is the oldest available genus group name for these fishes. Recently, this revalidation has been criticized (Schmidt & Bart Jr. 2015); we prefer, however, the use of *Enteromius* over '*Barbus*'.

The taxonomy of species of *Enteromius* is to date insufficiently known, resulting in difficulties in identifications and incomplete inventories of the species. It also hampers further studies on phylogenetic relationships, which are still obscure among species of *Enteromius* (Berrebi *et al.* 2014; Yang *et al.* 2015; Ren & Mayden 2016). While these problems have been tackled in various Asian taxa (Berrebi & Tsigenopoulos 2003; Pethiyagoda *et al.* 2012), the need for such revisions remains for the African species.

This study focuses on some species of *Enteromius* from the Congo basin. The Congo basin comprises the second largest catchment area in the world after the Amazon (Snoeks *et al.* 2011). It harbours a very high diversity of fishes with at least 957 valid species currently listed, excluding lakes Kivu and Tanganyika as well as the Malagarazi system (Froese & Pauly 2017; Musschoot, RMCA, pers. comm.). The Congo basin is generally divided into three main sections: the Upper Congo (or Lualaba), which runs from the basin's source in Zambia down to the Wagenia Falls near the city of Kisangani in north-eastern DR Congo; the Middle Congo, which starts at the Wagenia Falls, and flows in a large arc, first north-westwards, then southwards, before widening into Pool Malebo; and the Lower Congo, which starts at the outlet of Pool Malebo and runs down to the mouth of the basin in the Atlantic Ocean (Runge 2007). Despite the fact that the Congo basin is recognized as a hotspot for fish diversity (Snoeks *et al.* 2011), the ichthyofauna in large parts of the basin remains poorly studied. To date, 90 morphologically often very similar species of *Enteromius* are recognized from the Congo basin (Vreven, RMCA, pers. comm.). Identification keys for the region are lacking and the designation of so-called species complexes is the result of the identification difficulties. One of the specific taxonomic problems within the Congolese species of *Enteromius* concerns the *E. miolepis/eutaenia* complex, which comprises species characterized by a strongly ossified first dorsal ray that is serrated along its posterior margin and a blackish mid-lateral band that extends from the tip of the snout to the caudal fin base or onto the mid-central part of the caudal fin (Tweddle & Skelton 2008; Banyankimbona *et al.* 2012). Due to the similarity of the species within

this complex (Poll 1976), the available information on morphological characteristics is often insufficient to arrive at a correct species identification. In addition, *E. miolepis* (Boulenger, 1902) and *E. eutaenia* (Boulenger, 1904) are both characterized by high intraspecific morphological variation, which suggests that these taxa could be polyspecific. Some Congolese specimens were identified as *E. holotaenia* (Boulenger, 1904) or *E. kerstenii* (Peters, 1868), although both species were described from outside the Congo basin, from the Ogowe River in Gabon and from a coastal river in Zanzibar respectively. With their ossified, serrated dorsal spine and blackish mid-lateral band, they can be considered members of the *E. miolepis/eutaenia* complex. *Enteromius holotaenia* can only be distinguished from other members of the *E. miolepis/eutaenia* complex by the presence of a black dorsal fin tip, which is not always clearly visible, and *E. kerstenii* by the presence of a red opercular spot and the absence of large scales on the dorsal fin base. However, in the Congolese specimens identified as *E. kerstenii*, some enlarged scales seem to be present at the dorsal fin base, although not very pronounced.

In order to unravel the taxonomy of species of *Enteromius* from the Congo basin and delineate the various species, a morphologic approach alone may be inadequate. The present study ascertains whether a multidisciplinary approach might facilitate the differentiation of taxa within the genus *Enteromius* from the Congo basin. For this, some species of the north-eastern part of the basin, a particularly poorly explored region, were selected as a case study. Additionally, because of the taxonomic problems in the *E. miolepis/eutaenia* complex discussed above, we have examined specimens from this complex from other regions within the Congo basin as well. We explored whether this multidisciplinary approach would result in the discovery of cryptic species, and the detection of (additional) morphological characteristics to discriminate between these species.

To attain these objectives, we used DNA barcoding (Hebert *et al.* 2003) together with traditional morphometrical techniques. Molecular techniques like DNA barcoding have already proven to be powerful for the identification of both marine and freshwater fish taxa (Becker *et al.* 2011; Pereira *et al.* 2013), and to detect cryptic species diversity or taxonomic inconsistencies (Goodier *et al.* 2011; Collins & Cruickshank 2012; Decru *et al.* 2016). However, the uncritical use of molecular tools to identify species, especially using only a single molecular locus (mt genome), is unwarranted (DeSalle *et al.* 2011), and traditional morphology has proven its value as a suitable technique to assess the diversity in many taxa. Therefore, we combined both methodologies in the present study, an approach that has already proven to be successful in several taxonomic studies (e.g., Olayemi *et al.* 2012; Stiassny *et al.* 2013; Lavoué & Sullivan 2014).

Material & methods

Specimen selection (Fig. 2B, Table 1)

In total, we used 181 specimens of *Enteromius* from the Congo Basin for morphological and/or genetic analyses. To investigate the taxonomic diversity of *Enteromius* in the north-eastern part of the Congo basin (Middle Congo), we examined specimens of all species of *Enteromius* for which tissue samples had been recently collected from rivers in this region, i.e., the Ituri, its tributary the Epulu, the Lobilo, and the Lomami/Lobaye system. To unravel the *E. miolepis/eutaenia* complex, we also examined specimens from various sampling sites in the Upper, Middle and Lower Congo, identified as *E. miolepis, E. eutaenia, E. holotaenia* or *E. kerstenii.* For the Middle Congo, we included specimens from the Léfini, the Itimbiri, the Ituri/Epulu, the Lobilo, and the Lomami/Lobaye. For the Upper Congo we included samples from the Loboya (a tributary of the Maiko), and the Luapula. Finally, for the Lower Congo we used samples from the rivers Luki and Inkisi. These specimens were collected during ten expeditions that were carried out between 2005 and 2012.

Relevant types were selected based on the literature-based identifications and include the holotype of *E. miolepis* described from the Yembe River at Banzyville (Ubangi river system); 15 syntypes of *E. holotaenia* described from the Ogowe River in Gaboon; one lectotype and five paralectotypes of *E. eutaenia* described from Huila (Mossamedes) in Angola; the lectotype of *E. kerstenii* described from the coast opposite Zanzibar; the holotype of *E. brazzai* (Pellegrin, 1901) described from the Sangha River in Mobaka; the holotype and five paratypes of *E. tshopoensis* (De Vos, 1991), a junior synonym of *E. brazzai,* which was described from the Tshopo River; the lectotype and three paralectotypes of *E. pellegrini* (Poll, 1939) described from Lake Kivu; and two paratypes of *E. atromaculatus* (Nichols & Griscom, 1917) described from the Yakuluku River (Lévêque & Daget 1984) (see also Appendix 1).

We attempted to use the same specimens for the morphological and genetic analyses, but this was not always possible. As some specimens were lost or too damaged, 40 specimens that were genetically examined could not be used for morphological analyses. In 19 of these cases, literature-based identifications could not even be done, and the specimens were identified as *Enteromius* sp. As such, we morphologically examined 177 specimens (Table 1, Appendix 1), including several type specimens. Similarly, not all specimens that we examined morphologically could be successfully DNA barcoded, and genetic samples are unavailable for the type specimens.

Morphological analyses

Specimen identifications

Based on published characteristics, we assigned the non-type specimens to four 'a priori' groups: 60 to *E.* cf. *miolepis* (which represents the *E. miolepis/eutaenia* complex); 15 to *E.* cf. *brazzai*; 26 to *E.* cf. *pellegrini*; and 40 to *E.* cf. *atromaculatus*. We used 'cf.' to indicate the uncertainty connected to their identifications. The four groups mainly differ in the morphology of their dorsal spine (ossified or flexible; serrated or not) and colour pattern (Fig. 1). *Enteromius* cf. *miolepis* has an ossified serrated dorsal spine and a mid-lateral band on the flank and through the eye; *E.* cf. *brazzai* has a flexible unserrated dorsal spine and no melanin markings; *E.* cf. *pellegrini* has an ossified serrated dorsal spine and large dark

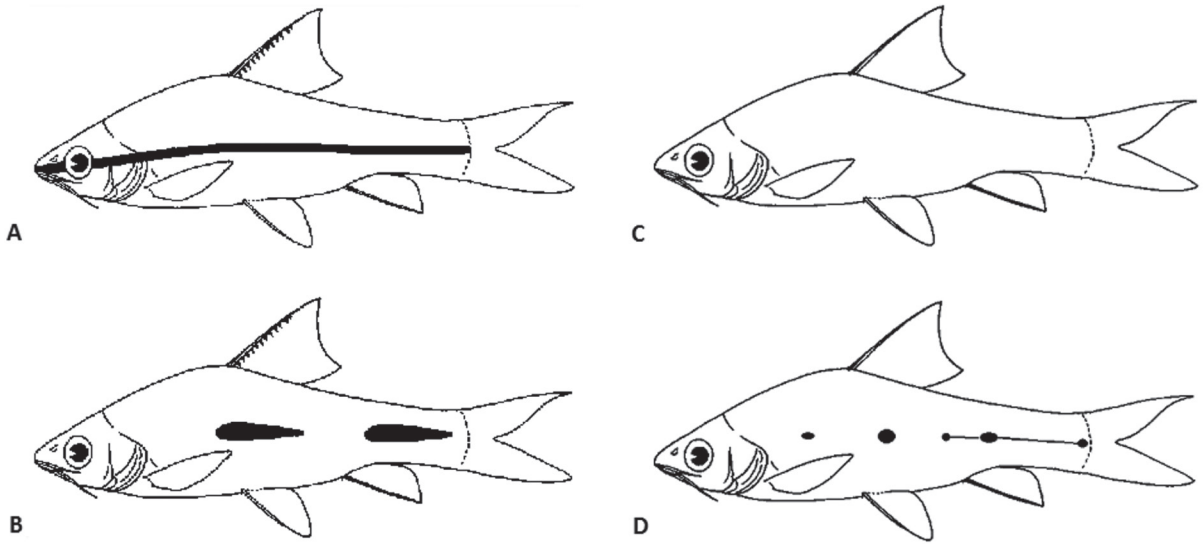

Fig. 1. Schematic representation of the four 'a priori' *Enteromius* groups with their characteristic morphological features (dorsal spine morphology and melanin pattern). **A**. *E.* cf. *miolepis* (Boulenger, 1902) (38.1–111.0 mm). **B**. *E.* cf. *pellegrini* (Poll, 1939) (40.7–81.3 mm). **C**. *E.* cf. *brazzai* (Pellegrin, 1901) (44.8–82.8 mm). **D**. *E.* cf. *atromaculatus* (Nichols & Griscom, 1917) (28.3–55.8 mm). Drawings modified from Bamba *et al.* (2011).

Table 1. Number of examined non-type specimens of *Enteromius* Cope, 1867 per river (system) studied. **A**. Specimens other than those belonging to the *E. miolepis/eutaniea* complex. **B**. Specimens belonging to the *E. miolepis/eutaenia* complex. Numbers represent morphometrically analysed specimens vs genetic samples, then the number of specimens analysed morphologically as well as genetically.

A

Region	River	Spec. examined (morphological/ genetical)	Spec. examined morphological & genetical
Middle Congo	Ituri	36/28	16
	Epulu (tributary Ituri)	32/7	7
	Lobilo	10/11	10
	Lobaye (tributary Lomami)	3/3	3

B

Upper Congo	Luapula	6/7	6
	Loboya (tributary Maiko)	0/1	0
Middle Congo	Léfini	5/5	5
	Itimbiri	2/2	2
	Ituri	6/13	4
	Epulu (tributary Ituri)	19/7	5
	Lobilo	4/7	4
	Lomami	1/1	1
	Lobaye (tributary Lomami)	4/4	3
Lower Congo	Inkisi	3/8	3
	Luki	10/10	5

spots that can fuse into a mid-lateral band; and *E.* cf. *atromaculatus* has a flexible unserrated dorsal spine and small spots that can fuse into a mid-lateral band.

Morphometry

For the 177 examined specimens, we obtained 17 measurements with a vernier caliper (Helios, 0.05 mm), as well as 10 meristics. Counts and measurements were based on Bamba *et al.* (2011), with some small modifications: the pre-occipital distance, post-dorsal distance I, post-anal distance I, and body-depth I were not included; the standard length, post-dorsal distance II, and post-anal distance II were measured up to the insertion of the first caudal fin ray of the upper lobe instead of to the middle of the caudal peduncle base. Barbel lengths were also coded according to Bamba *et al.* (2011). Head measurements were expressed as percentages of head length (HL) and body measurements as percentages of standard length (SL).

Abbreviations of the measurements and counts:

AFR = Anal fin rays
BD = Body depth
CP Sc = Caudal peduncle scales
DFR = Dorsal fin rays
D-L Sc = Scales dorsal fin-lateral line

DoFBL = Dorsal finbase length
DoFL = Dorsal fin length
ED = Eye diameter
HL = Head length
IOW = Interorbital width
L-B Sc = Scales lateral line-belly
LL Sc = Lateral line scales
L-P Sc = Scales lateral line-pelvic fin
MnCPD = Minimum caudal peduncle depth
MxCPD = Maximum caudal peduncle depth
PD Sc = Pre-dorsal scales
PecFR = Pectoral fin rays
PelFR = Pelvic fin rays
PoAD = Post-anal distance
PoDD = Post-dorsal distance
PrAD = Pre-anal distance
PrDD = Pre-dorsal distance
PrOpD = Pre-occipital distance
PrPecD = Pre-pectoral distance
PrPelD = Pre-pelvic distance
SL = Standard length
SnL = Snout length

Data analyses

We used principal component analysis to explore the multivariate data matrix and to reduce the large number of variables into a few meaningful axes (Snoeks 2004; Decru *et al.* 2012). PCAs were executed in Past 3.15c (Hammer *et al.* 2001). Raw data were used for meristics, log-transformations for the measurements. By using log-transformations, the first component can be interpreted as a proxy for size, since it is characterized by loadings with the same sign and same order of magnitude for all variables (Bookstein *et al.* 1985). Because the barbel lengths were coded (Bamba *et al.* 2011) as categorical variables, they were not included in the PCAs. PC loadings of the illustrated PCAs are given in the Appendices 2–8.

Genetic analyses

DNA Extraction, PCR amplification and sequencing

We successfully barcoded 114 specimens using DNA extracted from finclips (Table 1). The method used is based on the FISH-BOL (Fish Barcode of Life) protocol (Steinke & Hanner 2011). DNA was extracted using a 'NucleoSpin® Tissue Kit' following the instructions of the manufacturer (Macherey-Nagel, Germany). Subsequently, polymerase chain reactions (PCR) were used to amplify the mitochondrial cytochrome *c* oxidase I (COI) gene. A part of the samples was amplified with 'Fish Cocktail', an M13 tailed primer combination (Ivanova *et al.* 2007) (Table 2). A standard 25 µL PCR mix consisted of 2.5 µL PCR buffer (10x); 2.5 µL dNTP (2 mM); 1.25 µL 'Fish Cocktail' (2 µM); 0.2 Taq DNA Polymerase (5 units per µL); 16.75 µL mQ-H2O and 2.0 µL of the extracted DNA sample. The PCR profile was 3 min at 94°C, followed by 35 cycles of 40 s at 94°C, 40 s at 52°C, and 1 min at 72°C, plus a final extension of 10 min at 72°C. The success rate of this PCR-mix was relatively low, which led to the development of specific primers, Bbus F and Bbus R, for the amplification of samples that weren't successfully sequenced with 'Fish Cocktail' (Table 2). In this PCR mix, instead of 'Fish Cocktail', 2.5 µL of each specific primer was used, and an annealing temperature of 54°C instead of 52°C. Amplified products were verified on 1.2% agarose gels. Afterwards the PCR products were purified using a Nucleofast®

Table 2. Sequences 5'–3' of the primers used for the PCR reactions.

Name	Cocktail name / Primer sequence 5'–3'
	'Fish cocktail' (M13-tail): C_FishF1t1-C_FishR1t1 (ratio 1:1:1:1)
VF2_t1	TGTAAAACGACGGCCAGTCAACCAACCACAAAGACATTGGCAC
FishF2_t1	TGTAAAACGACGGCCAGTCGACTAATCATAAAGATATCGGCAC
FishR2_t1	CAGGAAACAGCTATGACACTTCAGGGTGACCGAAGAATCAGAA
FR1d_t1	CAGGAAACAGCTATGACACCTCAGGGTGTCCGAARAAYCARAA
Reference:	Ivanova *et al.* (2007)
	Primer sequences for M13-tails
M13F	TGTAAAACGACGGCCAGT
M13R	CAGGAAACAGCTATGAC
Reference:	Messing (1983)
	Primer sequences for *Enteromius* specific primers
Bbus F	TGAGCCGGAATAGTGGGAAC
Bbus R	CCTGCRGGGTCRAAGAATGT

96 PCR kit (Macherey-Nagel, Germany), and sequenced bidirectionally using BigDye Terminator v.3.1 and an ABI 3130 capillary sequencer.

DNA analyses

The DNA sequences were assembled and visually checked in CodonCode Aligner 5.1.4 (CodonCode Corporation) and aligned in MEGA 5.2 using Muscle Alignment (Edgar 2004; Tamura *et al.* 2011). The longer M13-sequences were shortened to the length of the Bbus-sequences (558 bp). Next, MEGA 5.2 was used to execute a model test and to create a phylogenetic tree. The model test indicated the GTR+G+I as the optimal model using the AIC criterion. This model was used to construct a Maximum-Likelihood (ML) tree with 1000 bootstrap replications. As both the ML tree and NJ (Neighbour Joining) tree gave similar results, statistical node support of both methods are visualised on the ML tree.

Results

Class Actinopterygii Klein, 1885
Subclass Neopterygii Regan, 1923
Division Teleostei Müller, 1846
Order Cypriniformes Rafinesque, 1810
Family Cyprinidae Rafinesque 1815

Genus ***Enteromius*** Cope, 1867

Evaluation of the literature-based identifications

In the ML tree obtained (Fig. 2), lineages with less than 2% sequence divergence were collapsed and named after the river system from which the specimens were collected. Specimens from the Lomami/Lobaye system and the Lobilo were grouped under the label 'Kisangani region', since there appeared to be little or no genetic difference between samples of these nearby affluents.

The ML tree shows 23 lineages within the assayed *Enteromius* samples, representing the four 'a priori' morphospecies in the following quantities/properties: 13 of which belong to the *E.* cf. *miolepis* group; three to the *E.* cf. *brazzai* group; one to the *E.* cf. *pellegrini* group; and six to the *E.* cf. *atromaculatus*

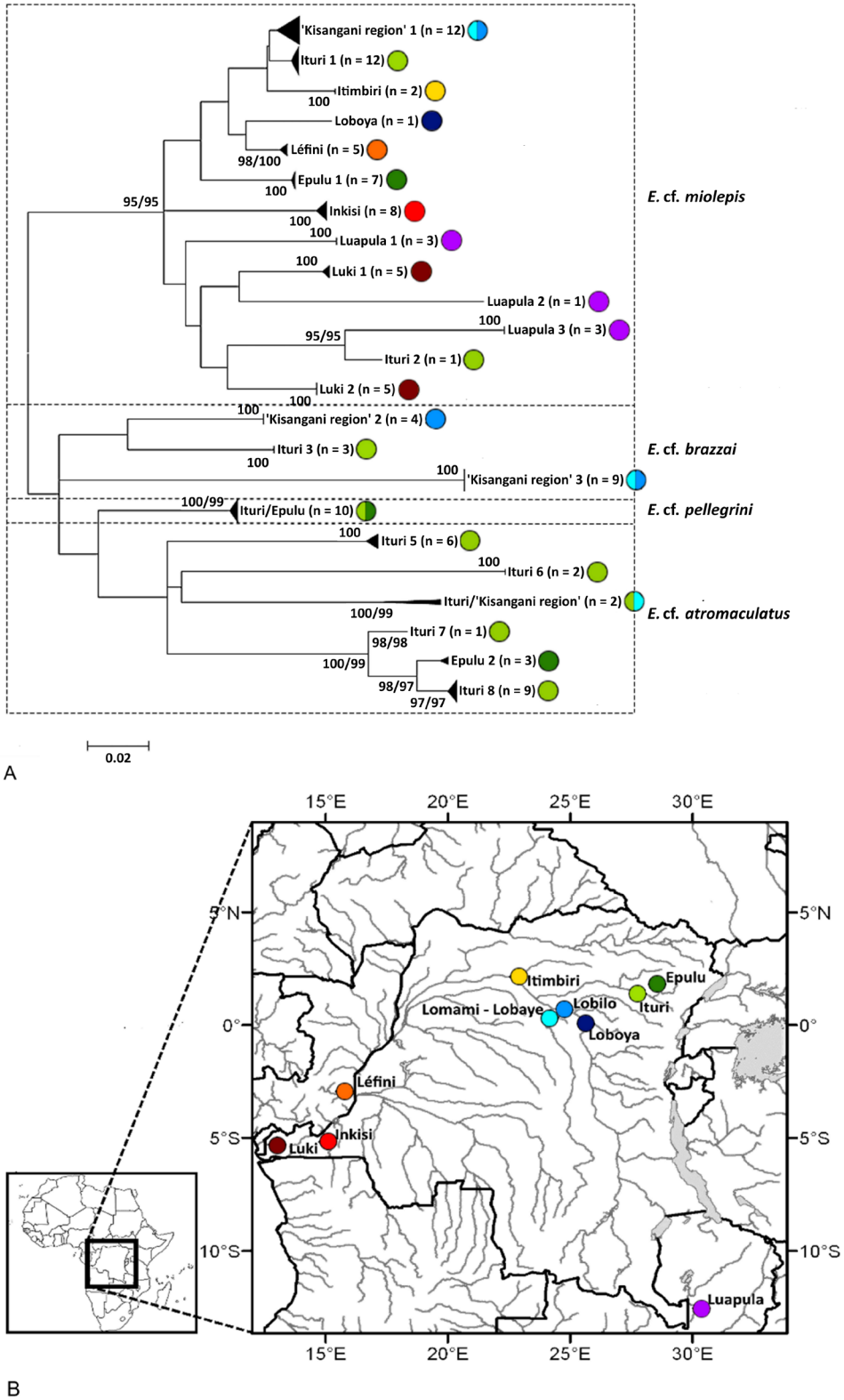

Fig. 2. A. ML tree based on 558-bp-long *Enteromius* COI sequences with 1000 bootstrap replications, with node support shown as NJ/ML bootstrap (bootstrap values > 95% are shown; lineages < 2% sequence divergence were collapsed), the label 'Kisangani region' contains samples from the Lomami/Lobaye system and the Lobilo. **B**. Map of the Congo basin with the sampled river stretches indicated according to the phylogenetic lineages.

group. *Enteromius* cf. *miolepis, E.* cf. *atromaculatus* and *E*. cf. *pellegrini* each form clearly supported clades, while this is not the case for *E.* cf. *brazzai*. There is often a substantial genetic distance between lineages occurring in different rivers, but also between some lineages detected in the same river. For example, within the *E.* cf. *miolepis* group, we observed a considerable difference between specimens of the Luapula (three lineages; 14.6% sequence divergence between Luapula 1 and 2; 15.3% between Luapula 1 and 3; 19.0% between Luapula 2 and 3), and the Luki (two lineages; 7.7% sequence divergence). Interestingly, the sequences obtained for the Upper, Middle and Lower Congo populations did not group according to these zoogeographic regions. However, two out of the three lineages of the Luapula, a river system geographically remote from the other rivers included in this study, also show the largest genetic distances within the *E.* cf. *miolepis* clade. *Enteromius* cf. *brazzai* is not resolved as a single clade, and consists of three lineages, two of which were detected in the 'Kisangani region' (19.8% sequence divergence). In contrast to the other groups, *E*. cf. *pellegrini* consists of a single lineage that is composed of specimens from a single river, the Ituri. The *E*. cf. *atromaculatus* group contains an important amount of genetic variation, with five of its six lineages occurring in the Ituri River. Remarkably, one of those lineages also contains one sample from the 'Kisangani region'.

Morphometric groupings

Firstly, PCAs were executed on all the specimens examined, after which more detailed PCAs were performed on each literature-based 'a priori' group separately.

Overall analyses

The highest loadings on PC2 for a PCA on 17 log-transformed measurements (n = 177) are for the eye diameter (ED), the post-anal distance (PoAD) and the dorsal fin length (DoFL); PC1 is a proxy for size (see above). On a scatterplot of PC2 against PC1, the four 'a priori' groups cannot all be distinguished from each other (Fig. 3). However, specimens of *E.* cf. *pellegrini* and *E.* cf. *brazzai* are completely separated from each other on PC2. This is mainly because *E.* cf. *pellegrini* has a smaller ED, a smaller dorsal fin base length (DoFBL) and a smaller PoAD than *E.* cf. *brazzai*. Clearly *E.* cf. *miolepis* occupies the largest morphospace on PC2, which comprises most of the type specimens included, except for two paralectotypes of *E. eutaenia* and one syntype of *E. holotaenia*. The *E.* cf. *atromaculatus* polygon comprises the paratypes of *E. atromaculatus*. The specimens of *E.* cf. *pellegrini*, however, only overlap slightly with the type specimens of *E. pellegrini* and the specimens of *E.* cf. *brazzai* are separated from the holotype of *E. brazzai* and types of *E. tshopoensis*. Furthermore, the type specimens of *E. tshopoensis* are separated from the other groups, mainly on PC2, due to a smaller PoAD and a larger DoFL.

The highest loadings on PC1 for a PCA on 10 meristics (n = 177) are for the number of scales between the lateral line and the belly (L-B Sc), the number of scales between the dorsal fin and the lateral line (D-L Sc) and the number of scales between the lateral line and the pelvic fin (L-P Sc); on PC2 for the number of scales on the lateral line (LL Sc), the number of scales between the occiput and the base of the first dorsal fin ray (PD Sc) and the number of pelvic fin rays (PelFR). Similar to the analysis for the measurements, a scatterplot of PC2 against PC1 does not allow the separation of the four 'a priori' groups (Fig. 4). Again, *E.* cf. *miolepis* is the group showing the largest variation. Also, *E.* cf. *pellegrini* and *E.* cf. *brazzai* are again completely separated on PC1, mainly due to *E.* cf. *pellegrini* having a higher D-L Sc (4.5–5.5 vs 3.5) and a higher L-B Sc (5–6 vs 4–5). Furthermore, the four 'a priori' groups all overlap with their respective type specimens.

To examine whether morphological differences could be detected between the different genetic lineages within each group, we performed PCAs on *E.* cf. *miolepis, E.* cf. *brazzai* and *E.* cf. *atromaculatus* separately. To investigate whether one or more lineages represent a currently valid species, relevant type

specimens were also included in these analyses. This resulted in a multitude of analyses for which the most important outcomes are presented below.

Morphometric comparisons among *E.* cf. *miolepis* lineages

Because of the high number of lineages and specimens for *E.* cf. *miolepis,* we analysed the major geographical regions, the Upper, the Middle and the Lower Congo, separately (see also Table 1), but still included the relevant type specimens to check whether some groups could be allocated to these species. Only the results of the latter are discussed as an example.

For the Lower Congo, we detected three genetic lineages within *E.* cf. *miolepis* (Fig. 2), i.e., one group containing specimens from the Inkisi and two groups with specimens from the Luki (Luki 1 and Luki 2). The highest loadings on PC1 for a PCA on 10 meristics (n = 36) are for LL Sc, CP Sc and PecFR; on PC2 again for PecFR, AFR and PD Sc. The specimens from the Inkisi are well separated from the Luki lineages on both PC1 and PC2; and there is only one specimen overlap between Luki 1 and Luki 2 (Fig. 5). In addition, specimens from these latter two lineages noticeably differ in the length of their barbels. Lineages Inkisi and Luki 1 can be clearly distinguished from all type specimens (Fig. 5). Luki 2 overlaps with the type specimens of *E. eutaenia* and *E. holotaenia*, but Luki 2 differs from the *E. eutaenia* types in barbel length. A PCA of the log-transformed measurements did not separate the genetic lineages from each other or from the type specimens (not illustrated).

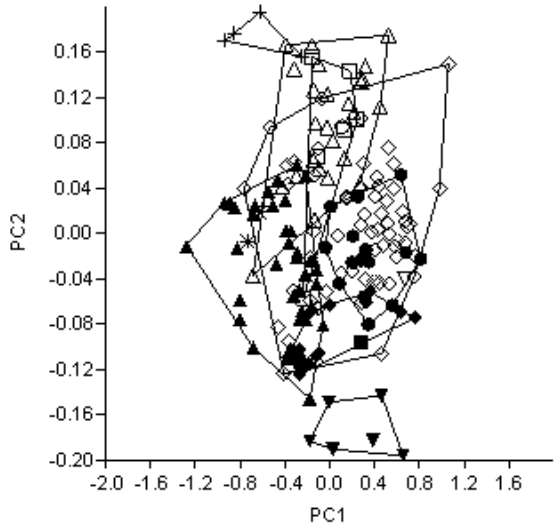

Fig. 3. Scatterplot of PC2 against PC1 for a PCA on 17 log-transformed measurements (n = 177) of *Enteromius* Cope, 1867: *E.* cf. *miolepis* (Boulenger, 1902) (◊), *E.* cf. *brazzai* (Pellegrin, 1901) (♦), *E.* cf. *pellegrini* (Poll, 1939) (Δ), and *E.* cf. *atromaculatus* (Nichols & Griscom, 1917) (▲). Also shown are the type specimens examined of: *E. miolepis* (Boulenger, 1902) (○), *E. holotaenia* (Boulenger, 1904) (●), *E. eutaenia* (Boulenger, 1904) (□), *E. kerstenii* (Peters, 1868) (■), *E. brazzai* (Pellegrin, 1901) (▽), *E. tshopoensis* (De Vos, 1991) (▼), *E. pellegrini* (Poll, 1939) (+), and *E. atromaculatus* (Nichols & Griscom, 1917) (✳).

For the Middle Congo and Upper Congo, we detected respectively six and four genetic lineages of *E.* cf. *miolepis* (Fig. 2). Similar exploratory morphometric analyses of these genetic lineages, as for the Lower Congo discussed above, indicated that almost all could be separated from each other as well as from the included type specimens. However, specimens from 'Kisangani region' 1, Itimbiri and the syntypes of *E. holotaenia* clustered on the PCAs. Yet, the Itimbiri specimens had a different colour pattern (a black anal fin tip), which is absent in the 'Kisangani region' 1 specimens as well as in the syntypes of *E. holotaenia*.

When comparing all lineages of *E.* cf. *miolepis* (Lower, Middle and Upper Congo), each could be morphologically distinguished from the others based on meristics (Fig. 6), measurements and/or barbel length (not illustrated). Only specimens from Kisangani region' 1 and Itimbiri could not be separated from each other, but differed in colour pattern (see above).

Morphometric comparisons among *E.* cf. *brazzai* lineages

We observed three genetic lineages within *E.* cf. *brazzai* (Fig. 2). The highest loadings on PC1 for a PCA on 10 meristics (n = 22) are for LL Sc, PecFR and PelFR; on PC2 for CP Sc, L-B Sc and again PecFR. Specimens from the 'Kisangani region' 2 are well separated from the Ituri 3 lineage on PC2 and both genetic lineages differ from the 'Kisangani region' 3 lineage and type specimens on PC1 (Fig. 7). The polygon of specimens from the 'Kisangani region' 3 lineage comprises the holotype of *E. brazzai* and overlaps with the types of *E. tshopoensis*. However, the eight specimens from the 'Kisangani region' 3

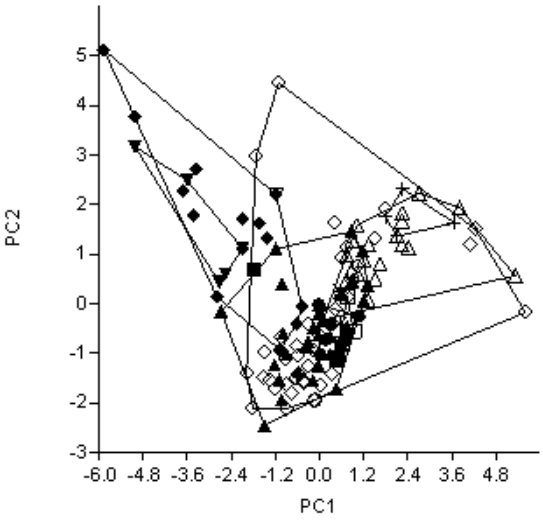

Fig. 4. Scatterplot of PC2 against PC1 for a PCA on 10 meristics (n = 177) of *Enteromius*: *E.* cf. *miolepis* (Boulenger, 1902) (◊), *E.* cf. *brazzai* (Pellegrin, 1901) (♦), *E.* cf. *pellegrini* (Poll, 1939) (Δ), and *E.* cf. *atromaculatus* (Nichols & Griscom, 1917) (▲). Also shown are the type specimens examined of: *E. miolepis* (Boulenger, 1902) (○), *E. holotaenia* (Boulenger, 1904) (●), *E. eutaenia* (Boulenger, 1904) (□), *E. kerstenii* (Peters, 1868) (■), *E. brazzai* (Pellegrin, 1901) (▽), *E. tshopoensis* (De Vos, 1991) (▼), *E. pellegrini* (Poll, 1939) (+), and *E. atromaculatus* (Nichols & Griscom, 1917) (✳).

lineage as well as the holotype of *E. brazzai* differ from the types of *E. tshopoensis* by the absence of barbels.

Morphometric comparisons among *E.* cf. *atromaculatus* lineages

We detected six genetic lineages within *E.* cf. *atromaculatus* (Fig. 2). Although there was only 1.75% sequence divergence between the lineages of Epulu 2 and Ituri 8, we interpreted these lineages as separate Operational Taxonomic Units (OTUs, i.e., clusters of similar DNA sequences) because of the observed differences in colour pattern (specimens from the Epulu 2 lineage have mid-lateral dots, while specimens from Ituri 8 display a vague mid-lateral band). The single specimen from Ituri 7 was lost and could not be measured. The highest loadings on PC1 for a PCA of 10 meristics (n = 42) are for LL Sc, PecFR and D-L Sc; on PC2 for CP Sc, again PecFR and D-L Sc. A plot of PC2 vs PC1, separates the two specimens from the Ituri 6 lineage from all other lineages based on PC2 (Fig. 8). The specimens from the Ituri/'Kisangani region' lineage are separated from all other lineages mainly on PC1. The Ituri 5 lineage is separated from the Ituri 6 and Epulu 2 lineages along PC2, from the *E. atromaculatus* type specimens on PC1, and from the Ituri/'Kisangani region' and Ituri 8 lineages on a combination of PC1 and PC2.

As the initial PCA resulted in a great overlap between the Epulu 2 and Ituri 8 lineages, we carried out a second PCA on 10 meristics, only including specimens from these lineages and the types of *E. atromaculatus*. The highest loadings on PC1 are for LL Sc, D-L Sc and CP Sc; on PC2 for PecFR, PD Sc and the number of pelvic fin rays (PelFR). On a plot of PC2 versus PC1, specimens from Epulu 2 and Ituri 8 still overlap and the types of *E. atromaculatus* overlap with specimens from Epulu 2 (Fig. 9). These groups also overlap on a PCA of 17 log-transformed measurements (not illustrated).

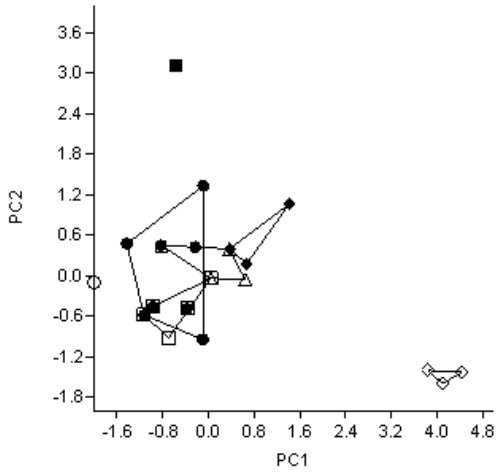

Fig. 5. Scatterplot of PC2 against PC1 for a PCA on 10 meristics (n = 36) of *E.* cf. *miolepis* specimens from the Lower Congo: Inkisi (◊), Luki 1 (♦) and Luki 2 (Δ). Also shown are the type specimens examined of: *E. miolepis* (Boulenger, 1902) (○), *E. holotaenia* (Boulenger, 1904) (●), *E. eutaenia* (Boulenger, 1904) (□) and *E. kerstenii* (Peters, 1868) (■).

Discussion

Multidisciplinary approach to detect cryptic species

Specimens from the genus *Enteromius* are notoriously difficult to identify. As, apart from some regional reviews (e.g., Bamba 2012), no extensive continent-wide reviews have been carried out for this genus, the available literature for species identifications is often limited to the accounts of the original species descriptions. Recent molecular studies already revealed *Enteromius* to be non-monophyletic (Yang *et al*. 2015; Ren & Mayden 2016).

Our study examined whether a multidisciplinary approach could provide more insight into the taxonomy of some species of *Enteromius* from the Congo basin and whether it might reveal cryptic diversity. For the examined species in this study, a literature-based identification led to the delineation of four so-called 'a priori' species. The reliability of these 'a priori' identifications was tested using a combined approach that consisted of DNA barcoding and a detailed morphometric approach that allowed the comparison of the specimens from our collection with relevant type specimens.

This approach revealed a high number of potentially new species of *Enteromius* within the examined samples/specimens. DNA barcoding uncovered the existence of 23 genetic lineages within the four 'a priori' species obtained by literature-based identifications. The genetic distances between many of the lineages, even within the 'a priori' species, were substantial. Sometimes they even reached almost 20%, which is considerably larger compared to most other African freshwater fish taxa, that usually have

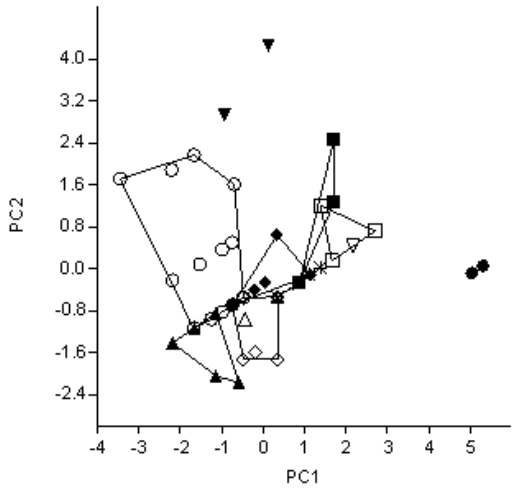

Fig. 6. Scatterplot of PC2 against PC1 for a PCA on 8 meristics (n = 60) of *E.* cf. *miolepis* (Boulenger, 1902) specimens from the Congo basin (excluding types): 'Kisangani region' 1 (◊), Ituri 1 (♦), Itimbiri (Δ), Lefini (▲), Epulu 1 (○), Inkisi (●), Luapula 1 (□), Luki 1 (■), Luapula 2 (▽), Luapula 3 (▼), Ituri 2 (+), and Luki 2 (✳). Specimens from Luapula 1 and Luapula 2 can be separated from each other based on a PCA on the log-transformed measurements; specimens of Luki 2 fall separated when barbel lengths are included; specimens from Kisangani region' 1 and Itimbiri can be distinguished based on colour pattern.

interspecific divergences lower than or around 10% for the COI gene (see, e.g., Lowenstein *et al.* 2011; Decru *et al*. 2016). Only three of the four 'a priori' species agreed with supported clades in our ML tree, i.e., *E.* cf. *miolepis, E.* cf. *pellegrini* and *E.* cf. *atromaculatus*, while the lineages of *E.* cf. *brazzai* do not form a supported clade. Subsequent exploratory morphometric analyses revealed that, despite the small sample sizes, most lineages could be separated on the basis of their morphology. The fact that specimens from separate genetic lineages are morphologically distinguishable, suggests that they may represent different species. Therefore, our hypothesis that at least the *E. miolepis/eutaenia* complex represents a polyspecific complex appears to be confirmed by our results, as within *E.* cf. *miolepis* we detected no less than 13 putative species. Also in the ML tree of Ren & Mayden (2016), samples from the *E. miolepis/eutaenia* complex formed five distinct lineages, three identified as *E. kerstenii,* one as *E. miolepis,* and one as *E. holotaenia.* Furthermore, respectively three and six putative species were detected in the 'a priori' species *E.* cf. *brazzai* and *E.* cf. *atromaculatus*. Interestingly, one of the important differences between the *E. cf. brazzai* lineages was the number of branched pelvic fin rays (7 vs 8). As far as we are aware, variation in the number of pelvic fin rays is uncommon in *Enteromius. Enteromius* cf. *pellegrini* is the only 'a priori' species that appears to be monospecific within the study area.

Providing formal descriptions with diagnoses of the undescribed species of *Enteromius* lies outside the scope of the present study, as it requires a detailed morphological examination of more specimens of each OTU and from other areas to unequivocally delineate species-specific diagnostic characteristics. In some analyses, type specimens ended up within or very close to the polygon of a particular OTU: the types of *E. holotaenia* partially overlapped with two OTUs of *E.* cf. *miolepis,* i.e., Luki 2 and 'Kisangani region' 1; the holotype of *E. brazzai* fell within an OTU of *E.* cf. *brazzai* from the Kisangani region ('Kisangani region' 3); and the types of *E. atromaculatus* overlapped with an OTU of *E.* cf. *atromaculatus* from the Epulu (Epulu 2). However, this does not necessarily imply that the OTUs are conspecific with the respective types. Our results indicated that in almost every studied river stretch at least one distinct species of *Enteromius* occurs, which makes it very unlikely that one of our studied OTUs from the Congo basin indeed represents *E. holotaenia,* a species originally described from the Ogowe River in the Lower Guinea ichthyofaunal province. Most of the specimens examined lacked the

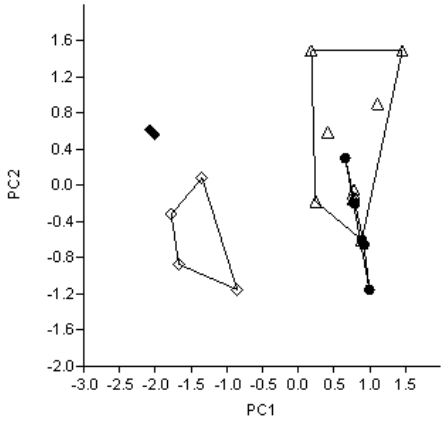

Fig. 7. Scatterplot of PC2 against PC1 for a PCA on 10 meristics (n = 22) of *E.* cf. *brazzai* (Pellegrin, 1901): 'Kisangani region' 2 (◊), Ituri 3 (♦) and 'Kisangani region' 3 (Δ). Also shown are the type specimens examined of *E. brazzai* (Pellegrin, 1901) (○) and *E. tshopoensis* (De Vos, 1991) (●).

black dorsal tip present in *E. holotaenia.* However, it was present in most of the specimens from Luki 2, in two of the nine specimens examined from 'Kisangani region 1', in both specimens from Itimbiri 1 and in one of the five specimens from the Lékini. This demonstrates that this feature is not consistently present in the lineages. Hence, it does not seem a good criterion for species to distinguish these taxa, also because this characteristic is paraphyletic in the ML tree (Fig. 2).

For *E. atromaculatus* and *E. brazzai* the situation appears to be different. *Enteromius atromaculatus* is described from the Yakuluku River (Uele River), which is in the vicinity of the Epulu River; and *Enteromius brazzai* is described from the Sangha River, which is also part of the Middle Congo. It is therefore plausible that the Epulu 2 population is conspecific with *E. atromaculatus,* and that 'Kisangani region' 3 is conspecific with *E. brazzai.* This implies that at least 21 of our 23 OTUs may represent new species that will need to be formally described in the future.

Distribution patterns and speciation processes

All species to which the specimens were originally assigned are presumed to have large distribution ranges that, except for *E. atromaculatus*, extend beyond the Congo basin. These wide distribution ranges of the four 'a priori' species on the one hand, and the often much narrower distribution ranges of the putative new species detected through DNA barcoding on the other, may be a reason why up to now, these OTUs were not detected as different species. Indeed, as the majority of earlier studies on ichthyofaunal diversity concern collections from small areas and even individual rivers, the studied specimens are often identified as one of the morphologically similar species presumed to occur in the studied region. Unfortunately, these identifications rarely imply detailed comparisons with specimens from other regions, let alone type specimens. In our study, most of the sympatric lineages were morphologically clearly distinct, and were as such already assigned to different 'a priori' species. In addition, the allopatric lineages within each of these 'a priori' species were morphologically sufficiently similar to remain grouped for as long as they were not subjected to comparisons based on multivariate morphometric methods. Although minor morphological differences can be interpreted as intraspecific geographic

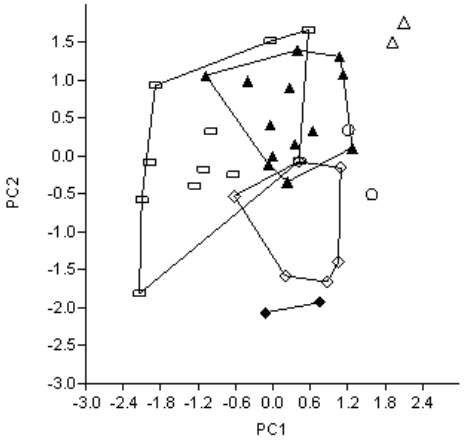

Fig. 8. Scatterplot of PC2 against PC1 for a PCA on 10 meristics (n = 42) of *E.* cf. *atromaculatus* (Nichols & Griscom, 1917): Ituri 5 (◊), Ituri 6 (♦), Ituri/'Kisangani region' (Δ), Epulu 2 (▲), and Ituri 8 (▬). Also shown are the type specimens of *E. atromaculatus* (Nichols & Griscom, 1917) (○).

variation among different populations, the detected morphological and genetic differences among the examined specimens of *Enteromius*, suggests that these populations probably represent separate, undescribed species. Although DNA barcodes allowed for the clustering of putative conspecifics, the obtained tree does not necessarily reflect the phylogenetic relationships within the genus *Enteromius*. A review of the phylogeny would not only require a comprehensive sampling of all species of *Enteromius* (some 200 species), but also the inclusion of outgroups. Nevertheless, some scenarios can be proposed concerning their evolutionary history. As in each of the geographically isolated river stretches studied distinct putative species appear to occur, allopatric speciation may well have been the main mode of speciation in this genus. However, the phylogenetic relationships among the species remain largely unresolved, as there is a lack of resolution in several parts of the ML tree. While it is possible that the lack of resolution is due to incomplete taxon sampling and/or to the small number of characters, we suggest a plausible cause to be rapid radiation, which often results in difficulties in resolving phylogenetic patterns (Fernández & Vrba 2005; Koblmüller *et al.* 2010). The unresolved phylogenies would in that case be the result of an almost concurrent differentiation between populations from different river stretches on a short evolutionary timescale. The fact that in this scenario adaptation to different niches has not been necessary, could thus be the cause that only minor morphological differences exist, which were only detected after multivariate exploratory techniques.

For *E.* cf. *atromaculatus* and *E.* cf. *pellegrini*, the populations from the Ituri River and its most important right-bank affluent, the Epulu River, have a slightly different colour pattern, which seems to support the scenario of allopatric speciation. However, for *E.* cf. *atromaculatus*, there was only a genetic divergence of 1.75% between these populations (Epulu 2 and Ituri 8 on Fig. 2A), and even no divergence for *E.* cf. *pellegrini* (Ituri/Epulu on Fig. 2A). Also based on counts and measurements, both populations of *E.* cf. *atromaculatus* (e.g., Figs 8–9) and *E*. cf. *pellegrini* (not illustrated) overlap. These two instances could be examples of intraspecific geographical colour variation rather than of two separate species in each of the two groups. This conclusion is unexpected, since even morphologically very similar populations were found to represent separate putative species in almost every individual river stretch. The observation that the populations from the Ituri and the Epulu cannot be distinguished based on the

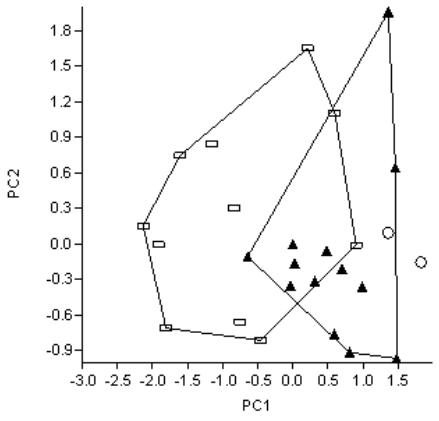

Fig. 9. Scatterplot of PC2 against PC1 for a PCA on 10 meristics (n = 36) of *E.* cf. *atromaculatus* (Nichols & Griscom, 1917): Epulu 2 (▲), and Ituri 8 (▬). Also shown are the type specimens of *E. atromaculatus* (Nichols & Griscom, 1917) (○).

multivariate analyses and do not appear to be genetically distinct, is even more surprising since these two river stretches are isolated. Indeed, the discussed populations are separated from each other by the presence of two waterfalls, one on the Epulu, just upstream of its confluence with the Ituri, and one on the Ituri itself (Vreven, RMCA, pers. comm.). These falls could form important barriers for fish species and populations, at least for upstream dispersal. However, this hypothesis does not appear to be supported by our results.

Interestingly, in some rivers multiple lineages of the same 'a priori' species appear to co-exist. This implies that in some instances morphologically similar putative (a posteriori) species may occur in sympatry; this is, e.g., the case for three lineages of *E.* cf. *miolepis* in the Luapula and two in the Luki River. Why morphologically very similar but separate species have evolved in the same rivers cannot be inferred from the present data set, and would require a phylogenetic analysis on multiple genetic markers and, e.g., additional information on ecology.

The distribution patterns, in combination with morphological (dis)similarities and the unresolved phylogenetic relationships, indicate that multiple allopatric speciation events on a short evolutionary timescale is a plausible mode of speciation for the examined species of *Enteromius*. Such allopatric divergences can occur in river systems when hydrological changes cause (simultaneous) disconnections of river stretches. Remarkably, some morphologically similar putative species occur however in sympatry.

Impact on documented species richness

By applying DNA barcoding in combination with multivariate analyses of morphometric data to several *Enteromius* populations from the Congo basin and the relevant type specimens, the number of species identified has increased from four based on literature to putatively 23. Considering the fact that only a part of the Congo basin and only some species have been studied, our results could imply a considerable increase of the number of species within this genus when extrapolated to the entire Congo basin or even Africa as a whole. A similar approach applied to other tropical vertebrates has yielded similar results. For instance, in a study on African giant pouched rats (*Cricetomys*, Nesomyidae), the combined use of DNA barcoding and cranial measurements lead to the discovery of at least three new species (Olayemi *et al.* 2012). Also for the fish genus *Pseudobarbus* (Cyprinidae) occurring in southern Africa, 15 separate lineages were identified, using cytb and 16S data, within the (at that time) seven valid species within the genus, most of which were confirmed by morphological results (Swartz *et al.* 2009). Also in Neotropical frogs, a study based on 16S rDNA indicated a huge underestimation of the current species richness, as up to 115% additional species were discovered (Fouquet *et al.* 2007). In the latter study however, no morphological analyses were performed to support the validity of the putative new species. These different studies indicate that not only for African fishes, but for several other vertebrate taxa in different regions on Earth, the current species richness could be severely underestimated. However, every case has its specific patterns, which indicates that a taxon-specific approach is needed for species detection and delineation. Systematically using a multidisciplinary approach could therefore result in an enormous increase of the overall documented species richness.

Correct insight in the number of species within a certain taxon is urgently needed to address conservation issues. When the number of species is highly underestimated, the decline of species may also be far worse than initially detected (Fouquet *et al.* 2007). Therefore, using molecular techniques can be of key importance for traditional taxonomy in accelerating the pace of species detection and description.

Acknowledgements

We would like to thank Koen De Gelas for his help in the lab as well as James Maclaine (NHM), Patrice Pruvost (MNHN) and Barbara Brown (AMNH) for the loan of type specimens under their care. We

are grateful to Emmanuel Vreven (RMCA) for providing literature-based compilations of the species of *Enteromius*, and for sampling the "Réserve de Faunes à Okapi", Epulu region and in the Ituri River; these expeditions were funded by the 'Leopold III-Fonds voor Natuuronderzoek en Natuurbehoud', 'Directorate-General for Development Cooperation and Humanitarian Aid' and the 'Stichting tot Bevordering van het Wetenschappelijk Onderzoek in Afrika'. The expedition to the Kisangani area in 2013 was funded by the BELSPO Science for a Sustainable Development (SSD) project entitled 'Congo basin: from carbon to fishes' (COBAFISH). This study is part of the PhD research of E.D., funded by a BELSPO action 2 programme.

References

Agnèse J.F., Berrebi P., Lévêque C. & Guégan J.F. 1990. Two lineages, diploid and tetraploid, demonstrated in African species *Barbus* (Osteichthyes, Cyprinidae). *Aquatic Living Resources* 3: 305–311. https://doi.org/10.1051/alr:1990031

Bamba M. 2012. *The* 'Barbus' *species (Cypriniformes, Cyprinidae) from Côte d'Ivoire: A Systematic Revision of Some West African Species Complexes*. PhD thesis, *KU Leuven, Belgium.*

Bamba M., Vreven E.J. & Snoeks J. 2011. Description of *Barbus teugelsi* sp. nov. (Cypriniformes: Cyprinidae) from the Little Scarcies basin in Guinea, Africa. *Zootaxa* 2988: 48–65.

Banyankimbona G., Vreven E. & Snoeks J. 2012. *'Barbus' devosi*, new species from the Malagarazi River basin in Burundi and Tanzania, East Africa (Cypriniformes: Cyprinidae). *Ichthyological Exploration of Freshwaters* 23: 181–192.

Becker S., Hanner R.H. & Steinke D. 2011. Five years of FISH-BOL: Brief status report. *Mitochondrial DNA* 22: 3–9. https://doi.org/10.3109/19401736.2010.535528

Berrebi P. & Tsigenopoulos C.S. 2003. Phylogenetic organization of the genus *Barbus* sensu stricto: A review based on data obtained using molecular markers. *In:* Bănărescu P.M. & Bogutskaya N.G. (eds) *The Freshwater Fishes of Europe Volume 5/II Cyprinidae 2, Part II: Barbus*: 11–22. Aula-Verlag, Wiesbaden.

Berrebi P. & Valiushok D. 1998. Genetic divergence among morphotypes of Lake Tana (Ethiopia) barbs. *Biological Journal of the Linnean Society* 64: 369–384. https://doi.org/10.1111/j.1095-8312.1998.tb00338.x

Berrebi P., Kottelat M., Skelton P. & Rab P. 1996. Systematics of *Barbus*: State of the art and heuristic comments. *Folia Zoologica* 45: 5–12.

Berrebi P., Chenuil A., Kotlik P., Machordom A. & Tsigenopoulos C.S. 2014. Disentangling the evolutionary history of the genus *Barbus sensu latu,* a twenty years adventure. *In:* Alves M.J., Cartaxana A., Correia A.M. & Lopes L.F. (eds) *Professor Carlos Almaça (1934–2010) – Estado da arte em áreas científicas do seu interesse*: 29–55. Museu Nacional de História Natural e da Ciência, Lisboa.

Bookstein F.L., Chernoff B., Elder R.L., Humphries J.M., Smith G.R. & Strauss R.E. 1985. *Morphometrics in Evolutionary Biology: the Geometry of Size and Shape Change, with Examples from Fishes*. Academy of Natural Sciences of Philadelphia, Philadelphia.

Collins R.A. & Cruickshank R.H. 2012. The seven deadly sins of DNA barcoding. *Molecular Ecology Resources* 13: 969–975. https://doi.org/10.1111/1755-0998.12046

Decru E., Vreven E. & Snoeks J. 2012. A revision of the West African *Hepsetus* (Characiformes; Hepsetidae) with a description of *H. akawo* sp. nov. and a redescription of *H. odoe* (Bloch, 1794). *Journal of Natural History* 46: 1–23. https://doi.org/10.1080/00222933.2011.622055

Decru E., Moelants T., De Gelas K., Vreven E., Verheyen E. & Snoeks J. 2016. Taxonomic challenges in freshwater fishes: a mismatch between morphology and DNA barcoding in fish of the north-eastern

part of the Congo basin. *Molecular Ecology Resources* 16: 342–352. https://doi.org/10.1111/1755-0998.12445

DeSalle R., Egan M.G. & Siddall M. 2011. The unholy trinity, taxonomy, species delimitation and DNA barcoding. *Philosophical Transactions of the Royal Society B* 360: 1905–1916. https://doi.org/10.1098/rstb.2005.1722

Edgar R.C. 2004. MUSCLE: multiple sequence alignment with high accuracy and high throughput. *Nucleic Acids Research* 32: 1792–1797. https://doi.org/10.1093/nar/gkh340

Fernández M.H. & Vrba E.S. 2005. A complete estimate of the phylogenetic relationships in Ruminantia: a dated species-level supertree of the extant ruminants. *Biological Reviews* 80: 269–302. https://doi.org/10.1017/s1464793104006670

Fouquet A., Gilles A., Vences M., Marty C., Blanc M. & Gemmell N.J. 2007. Underestimation of species richness in Neotropical frogs revealed by mtDNA analyses. *PLoS ONE* 2: e1109. https://doi.org/10.1371/journal.pone.0001109

Froese R. & Pauly D. 2017. FishBase. Available from www.fishbase.org [accessed 30 Mar. 2017].

Golubtsov A.S. & Krysanov E.Y. 1993. Karyological study of some cyprinid species from Ethiopia. The ploidy differences between large and small *Barbus* of Africa. *Journal of Fish Biology* 42: 445–455. https://doi.org/10.1111/j.1095-8649.1993.tb00347.x

Goodier S.A.M., Cotterill F.P.D., O'Ryan C., Skelton P.H. & de Wit M.J. 2011. Cryptic diversity of African Tigerfish (Genus *Hydrocynus*) reveals palaeogeographic signatures of linked Neogene geotectonic events. *PLoS ONE* 6: e28875. https://doi.org/10.1371/journal.pone.0028775

Hammer Ø., Harper D.A.T. & Ryan P.D. 2001. PAST: Paleontological statistics software package for education and data analysis. *Palaeontologia Electronica* 4: 1–9.

Hebert P.D.N., Cywinska A., Ball S.L. & de Waard J.R. 2003. Biological identifications through DNA barcodes. *Proceedings of the Royal Society B* 270: 313–321. https://doi.org/10.1098/rspb.2002.2218

Ivanova N.V., Zemlak T.S., Hanner R.H. & Hebert P.D. 2007. Universal primer cocktails for fish DNA barcoding. *Molecular Ecology Notes* 7: 544–548. https://doi.org/10.1111/j.1471-8286.2007.01748.x

Koblmüller S., Egger B., Sturmbauer C. & Sefc K.M. 2010. Rapid radiation, ancient incomplete lineage sorting and ancient hybridization in the endemic Lake Tanganyika cichlid tribe Tropheini. *Molecular Phylogenetics and Evolution* 55: 318–334. https://doi.org/10.1016/j.ympev.2009.09.032

Lavoué S. & Sullivan J.P. 2014. *Petrocephalus boboto* and *Petrocephalus arnegardi*, two new species of African electric fish (Osteoglossomorpha, Mormyridae) from the Congo River basin. *ZooKeys* 400: 43–65. https://doi.org/10.3897/zookeys.400.6743

Lévêque C. & Daget J. 1984. Cyprinidae. *In*: Daget J., Gosse J.P. & Van den Audenaerde T.D. (eds) *Check-list of the Freshwater Fishes of Africa (CLOFFA1)*: 217–342. ORSTOM & MRAC, Paris & Tervuren.

Lowenstein J.H., Osmundson T.Z., Becker S., Hanner R. & Stiassny M.L.J. 2011. Incorporating DNA barcodes into a multi-year inventory of the fishes of the hyperdiverse Lower Congo River, with a multi-gene performance assessment of the genus *Labeo* as a case study. *Mitochondrial DNA* 21: 1–19. https://doi.org/10.3109/19401736.2010.537748

Messing J. 1983. New M13 vectors for cloning. *Methods in Enzymology* 101: 20–78. https://doi.org/10.1016/0076-6879(83)01005-8

Oellermann L.K. & Skelton P.H. 1990. Hexaploidy in yellowfish species (*Barbus*, Pisces, Cyprinidae) from southern Africa. *Journal of Fish Biology* 37: 105–115. https://doi.org/10.1111/j.1095-8649.1990.tb05932.x

Olayemi A., Nicolas V., Hulselmans J.A.N., Missoup A.D., Fichet-Calvet E., Amundala D., Dudu A., Dierckx T., Wendelen W., Leirs H. & Verheyen E. 2012. Taxonomy of the African giant pouched rats (Nesomyidae: *Cricetomys*): molecular and craniometric evidence support an unexpected high species diversity. *Zoological Journal of the Linnean Society* 165: 700–719. https://doi.org/10.1111/j.1096-3642.2012.00823.x

Pereira L.H.G., Hanner R., Foresti F. & Oliveira C. 2013. Can DNA barcoding accurately discriminate megadiverse Neotropical freshwater fish fauna? *BMC Genetics* 14: 20. https://doi.org/10.1186/1471-2156-14-20

Pethiyagoda R., Meegaskumbura M. & Maduwage K. 2012. A synopsis of the South Asian fishes referred to *Puntius* (Pisces: Cyprinidae). *Ichthyological Exploration of Freshwaters* 23: 69–95.

Poll M. 1976. *Exploration du Parc National de l'Upemba Mission G.F. de Witte, 73: Poissons.* Fondation pour favoriser les recherches scientifiques en Afrique, Bruxelles.

Rab P., Machordom A., Perdices A. & Guegan J.F. 1995. Karyotypes of three «small» *Barbus* species (Cyprinidae) from Republic of Guinea (Western Africa) with a review on karyology of African small *Barbus*. *Caryologia* 48: 299–307. https://doi.org/10.1080/00087114.1995.10797339

Ren Q. & Mayden R.L. 2016. Molecular phylogeny and biogeography of African diploid barbs, '*Barbus*', and allies in Africa and Asia (Teleostei: Cypriniformes). *Zoologica Scripta* 45 (6): 642–649. https://doi.org/10.1111/zsc.12177

Runge J. 2007. The Congo River, Central Africa. *In*: Gupta A. (ed.) *Large Rivers: Geomorphology and Management*: 293–309. John Wiley & Sons Ltd, West Sussex.

Schmidt R.C. & Bart Jr. H.L. 2015. Nomenclatural changes should not be based on equivocally supported phylogenies: Reply to Yang *et al.* 2015. *Molecular Phylogenetics and Evolution* 90: 193–194. https://doi.org/10.1016/j.ympev.2015.05.025

Snoeks J. 2004. *The Cichlid Diversity of Lake Malawi/Nyassa/Niassa: Identification, Distribution and Taxonomy.* Cichlid Press, Texas.

Snoeks J., Harrison I.J. & Stiassny M.L.J. 2011. The status and distribution of freshwater fishes. *In*: Darwall W., Smith K., Allen D., Holland R., Harrison I. & Brooks E. (eds) *The Diversity of Life in African Freshwaters: Underwater, under Threat. An Analysis of the Status and Distribution of Freshwater Species throughout Mainland Africa*: 42–91. IUCN, Gland & Cambridge.

Steinke D. & Hanner R. 2011. The FISH-BOL collaborators' protocol. *Mitochondrial DNA* 22: 10–14. https://doi.org/10.3109/19401736.2010.536538

Stiassny M.L., Denton J.S. & Monsebula Iyaba R.J.C. 2013. A new ectoparasitic distichodontid of the genus *Eugnathichthys* (Characiformes: Citharinoidei) from the Congo basin of central Africa, with a molecular phylogeny for the genus. *Zootaxa* 3693: 479–490. https://doi.org/10.11646/zootaxa.3693.4.4

Swartz E.R., Skelton P.H. & Bloomer P. 2009. Phylogeny and biogeography of the genus *Pseudobarbus* (Cyprinidae): shedding light on the drainage history of rivers associated with the Cape Floristic Region. *Molecular Phylogenetics and Evolution* 51: 75–84. https://doi.org/10.1016/j.ympev.2008.10.017

Tamura K., Peterson D., Peterson N., Stecher G., Nei M. & Kumar S. 2011. MEGA5: molecular evolutionary genetics analysis using maximum likelihood, evolutionary distance, and maximum parsimony methods. *Molecular Biology and Evolution* 28: 2731–2739. https://doi.org/10.1093/molbev/msr121

Tsigenopoulos C.S., Kasapidis P. & Berrebi P. 2010. Phylogenetic relationships of hexaploid large-sized barbs (genus *Labeobarbus*, Cyprinidae) based on mtDNA data. *Molecular Phylogenetics and Evolution* 56: 851–856. https://doi.org/10.1016/j.ympev.2010.02.006

Tweddle D. & Skelton P.H. 2008. New species of '*Barbus*' and *Labeobarbus* (Teleostei: Cyprinidae) from the South Rukuru River, Malawi, Africa. *Smithiana Publications in Aquatic Biodiversity, Bulletin* 8: 25–39.

Yang L., Sado T., Hirt M.V., Pasco-Viel E., Arunachalam M., Li J., Wang X., Freyhof J., Saitoh K., Simons A.M., Miya M., He S. & Mayden R.L. 2015. Phylogeny and polyploidy: Resolving the classification of cyprinine fishes (Teleostei: Cypriniformes). *Molecular Phylogenetics and Evolution* 85: 97–116. https://doi.org/10.1016/j.ympev.2015.01.014

Manuscript received: 3 June 2016
Manuscript accepted: 24 August 2016
Published on: 12 April 2017
Topic editor: Rudy Jocqué
Desk editor: Kristiaan Hoedemakers

Appendix 1. List of the morphologically examined specimens. **A**. Non-type specimens. **B**. Type specimens.

A

Genetic lineage	Label	Collection	Location	SL (mm)
			E.* cf. *miolepis	
'Kisangani region' 1_1	0323	B0-09-P-0096	Riv. Lomami, left bank, Djabir, site 31 (00°28′30.4″ N, 24°09′47.8″ E)	52.85
'Kisangani region' 1_2	2912	B0-09-P-0088-0089	Riv. Lobaye, right bank, Djabir, site 6 (00°29′28.1″ N, 24°10′42.8″ E)	46.40
'Kisangani region' 1_3	2913	B0-09-P-0088-0089	Riv. Lobaye, right bank, Djabir, site 6 (00°29′28.1″N, 24°10′42.8″ E)	52.95
'Kisangani region' 1_4	6638	B0-21-P-0885-0886	Riv. Lobaye, right bank, Djabir, site 10 (00°29′25.2″ N, 24°10′40.3″ E)	58.60
'Kisangani region' 1_5	6639	B0-21-P-0885-0886	Riv. Lobaye, right bank, Djabir, site 10 (00°29′25.2″ N, 24°10′40.3″ E)	62.15
'Kisangani region' 1_6	12315	B3-30	Riv. Lobilo village Busukulu, right bank upstream of the Kibanguist mission	66.55
'Kisangani region' 1_7	12316	B3-30	Riv. Lobilo village Busukulu, right bank upstream of the Kibanguist mission	78.00
'Kisangani region' 1_8	12374	B3-30	Riv. Lobilo village Busukulu, right bank upstream of the Kibanguist mission	80.90
'Kisangani region' 1_9	12412	B3-30	Riv. Lobilo village Busukulu, right bank upstream of the Kibanguist mission	57.60
Ituri 1_1	/	B1-11-G-00466	Riv. Ebiena dowstream of the confluence with Lohulo P5	73.55
Ituri 1_2	/	B1-11-G-00495	Riv. Biakato-mayi, village Biakato-mayi upstream of the bridge	76.05
Ituri 1_3	/	B1-11-G-00496	Riv. Biakato-mayi, village Biakato-mayi upstream of the bridge	70.95
Ituri 1_4	/	B1-11	Riv. Loya near the bridge of the village	57.35
Ituri 1_5	/	B1-11	Riv. Loya near the bridge of the village	59.30
Itimbiri_1	4671	B0-17-P-0089	Riv. Kona, small tributary on the right bank of the Itimbiri, upstream the Kona camp	50.10
Itimbiri_2	4726	B0-17-P-0088	Riv. Kona, small tributary on the right bank of the Itimbiri, upstream the Kona camp	82.60
Léfini_1	0494	A7-31-P-0537	Riv. Léfini, confluence Léfini-Nambouli, left bank	69.50
Léfini_2	1106	A8-20-P-1059-1060	Riv. Léfini, downstream the Epopé mountain, right bank, +/- 2 km upstream of the PPG camp	83.15
Léfini_3	1107	A8-20-P-1059-1060	Riv. Léfini, downstream the Epopé mountain, right bank, +/- 2 km upstream of the PPG camp	65.25
Léfini_4	1465	A8-20-P-1073-1076	Riv. Louna, tributary of the Léfini, with rapids, left bank	42.15
Léfini_5	1482	A8-20-P-1090-1095	Riv. Louna, tributary of the Léfini, upstream of the rapids, right bank	77.30
Epulu 1_1	3052	A9-29-P-0952-0953	Riv. Mayi Mbili, small tributary of the Epulu, tributary of the Ituri (RFO)	76.30
Epulu 1_2	/	A9-029-P-0944-0951	Riv. Mayi Mbili, small tributary of the Epulu, tributary of the Ituri (RFO)	73.70
Epulu 1_3	/	A9-029-P-0944-0951	Riv. Mayi Mbili, small tributary of the Epulu, tributary of the Ituri (RFO)	44.00
Epulu 1_4	/	A9-029-P-0944-0951	Riv. Mayi Mbili, small tributary of the Epulu, tributary of the Ituri (RFO)	71.85
Epulu 1_5	/	A9-029-P-0944-0951	Riv. Mayi Mbili, small tributary of the Epulu, tributary of the Ituri (RFO)	65.70
Epulu 1_6	/	A9-029-P-0944-0951	Riv. Mayi Mbili, small tributary of the Epulu, tributary of the Ituri (RFO)	51.50

Epulu 1_7	/	A9-029-P-0944-0951	Riv. Mayi Mbili, small tributary of the Epulu, tributary of the Ituri (RFO)	69.75
Epulu 1_8	/	A9-029-P-0944-0951	Riv. Mayi Mbili, small tributary of the Epulu, tributary of the Ituri (RFO)	50.70
Epulu 1_9	/	A9-029-P-0944-0951	Riv. Mayi Mbili, small tributary of the Epulu, tributary of the Ituri (RFO)	43.25
Epulu 1_10	3476	A9-029-P-0776-0779	Riv. Lélo, close to the agricultural area of the centre of Epulu, tributary of the Epulu, bassin Ituri (RFO), in primary forest	68.70
Epulu 1_11	3477	A9-029-P-0776-0779	Riv. Lélo, close to the agricultural area of the centre of Epulu, tributary of the Epulu, bassin Ituri (RFO), in primary forest	77.25
Epulu 1_12	3483	A9-029-P-0776-0779	Riv. Lélo, close to the agricultural area of the centre of Epulu, tributary of the Epulu, bassin Ituri (RFO), in primary forest	78.00
Epulu 1_13	3484	A9-029-P-0776-0779	Riv. Lélo, close to the agricultural area of the centre of Epulu, tributary of the Epulu, bassin Ituri (RFO), in primary forest	87.15
Epulu 1_14	/	A9-029-P-0780-0796	Riv. Lélo, close to the agricultural area of the centre of Epulu, tributary of the Epulu, bassin Ituri (RFO), in primary forest	73.45
Epulu 1_15	/	A9-029-P-0780-0796	Riv. Lélo, close to the agricultural area of the centre of Epulu, tributary of the Epulu, bassin Ituri (RFO), in primary forest	77.80
Epulu 1_16	/	A9-029-P-0780-0796	Riv. Lélo, close to the agricultural area of the centre of Epulu, tributary of the Epulu, bassin Ituri (RFO), in primary forest	78.60
Epulu 1_17	/	A9-029-P-0780-0796	Riv. Lélo, close to the agricultural area of the centre of Epulu, tributary of the Epulu, bassin Ituri (RFO), in primary forest	70.70
Epulu 1_18	/	A9-029-P-0780-0796	Riv. Lélo, close to the agricultural area of the centre of Epulu, tributary of the Epulu, bassin Ituri (RFO), in primary forest	75.80
Epulu 1_19	/	A9-029-P-0780-0796	Riv. Lélo, close to the agricultural area of the centre of Epulu, tributary of the Epulu, bassin Ituri (RFO), in primary forest	72.80
Inkisi_1	611	A6-07-P-0486-0489	Riv. Ngufu, near the bridge of the village Luangu, Kavuaya, tributary of the Inkisi, Lower Congo	98.75
Inkisi_2	612	A6-07-P-0486-0489	Riv. Ngufu, near the bridge of the village Luangu, Kavuaya, tributary of the Inkisi, Lower Congo	83.80
Inkisi_3	613	A6-07-P-0486-0489	Riv. Ngufu, near the bridge of the village Luangu, Kavuaya, tributary of the Inkisi, Lower Congo	80.70
Luapula 1_1	1525	A8-21-P-0374-0376	Riv. Malaushi, riverside	47.25
Luapula 1_2	1531	A8-21-P-0385	Riv. Malaushi, bridge	69.55
Luapula 1_3	1665	A8-21-P-0429	Chantete, riv. Mulembo	110.95
Luki 1_1	545	A7-31-P-0912-0919	Riv. Luki, +/- 2.5 km of Kiwéléwélé	48.55
Luki 1_2	943	A7-31-P-0910-0911	Riv. Luki, near the bridge of the biosphere reserve of Luki	68.65
Luki 1_3	1062	A8-20-P-1384	Riv. Luki, near the bridge of the village Kiza	38.10
Luapula 2_1	1524	A8-21-P-0374-0376	Riv. Malaushi, riverside	43.80
Luapula 3_1	1635	A8-21-P-0472	Pontoon, riv. Kasanka, left bank	56.00
Luapula 3_2	1660	A8-21-P-0530	Katwa, riv. Kasanka	48.25
Ituri 2_1	/	B1-11-G-00543	Riv. Elake, village Elake upstream of the confluence with Ituri PN	57.05

Luki 2_1	0467	A6-07-P-0691-0692	Riv. Luki, upstream of the bridge in the Luki forest reserve, Lower Congo	66.80
Luki 2_2	0468	A6-07-P-0689	Riv. Luki, upstream of the bridge in the Luki forest reserve, Lower Congo	77.15
Luki 2_3	1037	A8-20-P-1368	Riv. Luki, confluence with the Lovo, several kms downstream of Kiwéléwélé	51.95
Luki 2_4	1065	A8-20-P-1369	Riv. Luki, upstream of the bridge at the vill. Kiza	70.00
Luki 2_5	/	A8-20-P-1371-1372	Riv. Luki, on the route of the camp upstream of the bridge	71.95
Luki 2_6	/	A8-20-P-1371-1372	Riv. Luki, on the route of the camp upstream of the bridge	67.05
Luki 2_7	/	A8-20-P-1370	Riv. Luki, upstream of the bridge at the vill. Kiza	53.80
			E.* cf. *brazzai	
Kisangani region' 2_1	12317	B3-30	Vill. Busukulu, riv. Lobilo, right bank upstream of the Kibanguist mission	76.95
Kisangani region' 2_2	12386	B3-30	Vill. Busukulu, riv. Lobilo, left bank upstream of the Kibanguist mission	82.80
Kisangani region' 2_3	12411	B3-30	Vill. Busukulu, riv. Lobilo, left bank upstream of the Kibanguist mission	68.10
Kisangani region' 2_4	12430	B3-30	Vill. Busukulu, riv. Lobilo, right bank upstream of the bridge	66.20
Ituri 3_1	3136	A9-29	Vill. Molokay, riv. Epene, downstream of the bridge	53.95
Ituri 3_2	3137	A9-29	Vill. Molokay, riv. Epene, downstream of the bridge	48.50
Ituri 3_3	3155	A9-29	Vill. Molokay, riv. Epene, downstream of the bridge	48.90
'Kisangani region' 3_1	8969	B3-30	Vill. Djatizi, riv. Lobaye, upstream of the fishing camp Likungu	55.00
'Kisangani region' 3_2	8970	B3-30	Vill. Djatizi, riv. Lobaye, upstream of the fishing camp Likungu	53.00
'Kisangani region' 3_3	12417	B3-30	Vill. Busukulu, riv. Lobilo, right bank upstream of the Kibanguist mission	49.80
'Kisangani region' 3_4	12418	B3-30	Vill. Busukulu, riv. Lobilo, right bank upstream of the Kibanguist mission	45.20
'Kisangani region' 3_5	12419	B3-30	Vill. Busukulu, riv. Lobilo, right bank upstream of the Kibanguist mission	48.00
'Kisangani region' 3_6	12420	B3-30	Vill. Busukulu, riv. Lobilo, right bank upstream of the Kibanguist mission	44.75
'Kisangani region' 3_7	12472	B3-30	Riv. Congo, downstream of the confluence with the Lobilo, right bank diagonally of Lotokila	49.35
'Kisangani region' 3_8	12477	B3-30	Riv. Congo, downstream of the confluence with the Lobilo, right bank diagonally of Lotokila	47.55
			E.* cf. *pellegrini	
Ituri/Epulu_1	3681	A9-029-P-0884-0885	Riv. Akokora, waterfalls of Koukou, tributary of the Epulu, bassin Ituri (RFO)	55.60
Ituri/Epulu_2	3682	A9-029-P-0884-0885	Riv. Akokora, waterfalls of Koukou, tributary of the Epulu, bassin Ituri (RFO)	57.85
Ituri/Epulu_3	/	A9-029-P-0886-0889	Riv. Akokora, waterfalls of Koukou, tributary of the Epulu, bassin Ituri (RFO)	58.75
Ituri/Epulu_4	/	A9-029-P-0886-0889	Riv. Akokora, waterfalls of Koukou, tributary of the Epulu, bassin Ituri (RFO)	55.50
Ituri/Epulu_5	/	A9-029-P-0886-0889	Riv. Akokora, waterfalls of Koukou, tributary of the Epulu, bassin Ituri (RFO)	62.20
Ituri/Epulu_6	/	A9-029-P-0886-0889	Riv. Akokora, waterfalls of Koukou, tributary of the Epulu, bassin Ituri (RFO)	54.65
Ituri/Epulu_7	3163	A9-029-P-0882-0883	Riv. Nepuse, small tributary of the Epulu in Epulu, bassin Ituri (RFO)	49.70
Ituri/Epulu_8	3164	A9-029-P-0882-0883	Riv. Nepuse, small tributary of the Epulu in Epulu, bassin Ituri (RFO)	50.75

Ituri/Epulu_9	/	A9-029-P-0881	Riv. Nepuse, small tributary of the Epulu in Epulu, bassin Ituri (RFO)	40.70
Ituri/Epulu_10	3214	A9-29-P-0966-0968	Riv. Nembongo, near the bridge on the route to Epulu, tributary of the Epulu, bassin Ituri (RFO)	57.90
Ituri/Epulu_11	3215	A9-29-P-0966-0968	Riv. Nembongo, near the bridge on the route to Epulu, tributary of the Epulu, bassin Ituri (RFO)	59.50
Ituri/Epulu_12	3216	A9-29-P-0966-0968	Riv. Nembongo, near the bridge on the route to Epulu, tributary of the Epulu, bassin Ituri (RFO)	54.80
Ituri/Epulu_13	/	A9-029-P-0963-0965	Riv. Nembongo, near the bridge on the route to Epulu, tributary of the Epulu, bassin Ituri (RFO)	51.00
Ituri/Epulu_14	/	A9-029-P-0963-0965	Riv. Nembongo, near the bridge on the route to Epulu, tributary of the Epulu, bassin Ituri (RFO)	43.95
Ituri/Epulu_15	/	A9-029-P-0963-0965	Riv. Nembongo, near the bridge on the route to Epulu, tributary of the Epulu, bassin Ituri (RFO)	47.05
Ituri/Epulu_16	/	A9-029-P-0890	Confluence Nduye-Biasa, downstream of the bridge of Nduye, tributary of the Epulu, bassin Ituri (RFO)	55.85
Ituri/Epulu_17	3603	A9-29-P-0891	Riv. Lolwa in Lolwa, upstream of the bridge, tributary of the Epulu	63.45
Ituri/Epulu_18	3613	A9-29-P-0892-0893	Riv. Lolwa in Lolwa, upstream of the bridge, tributary of the Epulu	81.35
Ituri/Epulu_19	3614	A9-29-P-0892-0893	Riv. Lolwa in Lolwa, upstream of the bridge, tributary of the Epulu	73.20
Ituri/Epulu_20	/	A9-029-P-0894-0900	Riv. Lolwa in Lolwa, upstream of the bridge, tributary of the Epulu	71.95
Ituri/Epulu_21	/	A9-029-P-0894-0900	Riv. Lolwa in Lolwa, upstream of the bridge, tributary of the Epulu	55.50
Ituri/Epulu_22	/	A9-029-P-0894-0900	Riv. Lolwa in Lolwa, upstream of the bridge, tributary of the Epulu	69.70
Ituri/Epulu_23	/	A9-029-P-0894-0900	Riv. Lolwa in Lolwa, upstream of the bridge, tributary of the Epulu	70.10
Ituri/Epulu_24	/	A9-029-P-0894-0900	Riv. Lolwa in Lolwa, upstream of the bridge, tributary of the Epulu	68.00
Ituri/Epulu_25	/	A9-029-P-0894-0900	Riv. Lolwa in Lolwa, upstream of the bridge, tributary of the Epulu	62.50
Ituri/Epulu_26	/	A9-029-P-0894-0900	Riv. Lolwa in Lolwa, upstream of the bridge, tributary of the Epulu	69.50
			E.* cf. *atromaculatus	
Ituri 5_1	3094	A9-029-P-0903-0904	Riv. Angolomu in Babeke, confluence with the Isaye, tributary of the Ituri (RFO)	51.55
Ituri 5_2	3095	A9-029-P-0903-0904	Riv. Angolomu in Babeke, confluence with the Isaye, tributary of the Ituri (RFO)	45.00
Ituri 5_3	3918	A9-029-P-0937-0940	Riv. Makulumba in Avakubi, small tributary of the Ituri, upstream of the bridge	44.80
Ituri 5_4	3919	A9-029-P-0937-0940	Riv. Makulumba in Avakubi, small tributary of the Ituri, upstream of the bridge	36.95
Ituri 5_5	3920	A9-029-P-0937-0940	Riv. Makulumba in Avakubi, small tributary of the Ituri, upstream of the bridge	37.65
Ituri 5_6	3921	A9-029-P-0937-0940	Riv. Makulumba in Avakubi, small tributary of the Ituri, upstream of the bridge	37.70
Ituri 6_1	3751	A9-029-P-0932	Riv. Ituri, across from the vill. Penge, downstream of the Penge rapids (RFO)	48.60
Ituri 6_2	3887	A9-029-P-0934-0935	Riv. Ituri in Avakubi, upstream of the bridge and the last rapids	48.45
Ituri 6_3	3888	A9-029-P-0934-0935	Riv. Ituri in Avakubi, upstream of the bridge and the last rapids	47.50
Ituri 6_4	/	A9-029-P-0936	Riv. Ituri in Avakubi, upstream of the bridge and the last rapids	50.60
Ituri/'Kisangani region'_1	3776	A9-029-P-0933	Riv. Ituri, upstream of the Penge rapids (RFO)	55.65
Ituri/'Kisangani region'_2	7325	B0-021-P-0883	Riv. Lobaye, right bank, Bonbandji II site 114 (00°11′33.6″ N, 25°31′51.1″ E)	44.30

Epulu 2_1	3037	/	Riv. Epulu in Epulu, right bank downstream of the bridge	47.15
Epulu 2_2	3038	/	Riv. Epulu in Epulu, right bank downstream of the bridge	48.50
Epulu 2_3	3055	A9-29-P-0901-0902	Riv. Mayi Mbili, small tributary of the Epulu, tributary of the Ituri (RFO)	35.75
Epulu 2_4	3056	A9-29-P-0901-0902	Riv. Mayi Mbili, small tributary of the Epulu, tributary of the Ituri (RFO)	34.00
Epulu 2_5	3205	/	Riv. Epulu, upstream of the bridge and across from chimpanzee island	41.00
Epulu 2_6	3206	/	Riv. Epulu, upstream of the bridge and across from chimpanzee island	44.20
Epulu 2_7	3555	A9-029-P-0908	Riv. Kaubeli, tributary of the Epulu in Bandisende, bassin Ituri	40.40
Epulu 2_8	/	A9-029-P-0906-0907	Riv. Kaubeli, tributary of the Epulu in Bandisende, bassin Ituri	28.25
Epulu 2_9	3667	A9-029-P-0909-0910	Riv. Nduye in Nduye, upstream of the last bridge behind the police camp, tributary of the Epulu, bassin Ituri (RFO)	51.45
Epulu 2_10	3668	A9-029-P-0909-0910	Riv. Nduye in Nduye, upstream of the last bridge behind the police camp, tributary of the Epulu, bassin Ituri (RFO)	51.50
Epulu 2_11	/	A9-029-P-0911-0913	Riv. Nduye in Nduye, upstream of the last bridge behind the police camp, tributary of the Epulu, bassin Ituri (RFO)	53.60
Epulu 2_12	/	A9-029-P-0911-0913	Riv. Nduye in Nduye, upstream of the last bridge behind the police camp, tributary of the Epulu, bassin Ituri (RFO)	50.80
Epulu 2_13	/	A9-029-P-0911-0913	Riv. Nduye in Nduye, upstream of the last bridge behind the police camp, tributary of the Epulu, bassin Ituri (RFO)	50.70
Epulu 2_14	3671	/	Riv. Uetefe in Nduye, right bank	36.25
Epulu 2_15	3685	A9-029-P-0919-0920	Riv. Akokora, waterfalls of Koukou, tributary of the Epulu, bassin Ituri (RFO)	54.85
Epulu 2_16	3686	A9-029-P-0919-0920	Riv. Akokora, waterfalls of Koukou, tributary of the Epulu, bassin Ituri (RFO)	55.75
Ituri 8_1	3317	A9-29-P-0954-0955	Riv. Bango in Bango, tributary of the Ituri	51.60
Ituri 8_2	3318	A9-29-P-0954-0955	Riv. Bango in Bango, tributary of the Ituri	45.95
Ituri 8_3	/	A9-029-P-0972-0973	Riv. Bango in Bango, upstream of the bridge along the mining operation, bassin Ituri	40.55
Ituri 8_4	/	A9-029-P-0972-0973	Riv. Bango in Bango, upstream of the bridge along the mining operation, bassin Ituri	45.70
Ituri 8_5	/	A9-029-P-0956-0962	Riv. Bango in Bango, tributary of the Ituri	46.05
Ituri 8_6	/	A9-029-P-0956-0962	Riv. Bango in Bango, tributary of the Ituri	47.15
Ituri 8_7	/	A9-029-P-0956-0962	Riv. Bango in Bango, tributary of the Ituri	51.35
Ituri 8_8	/	A9-029-P-0956-0962	Riv. Bango in Bango, tributary of the Ituri	49.90
Ituri 8_9	/	A9-029-P-0956-0962	Riv. Bango in Bango, tributary of the Ituri	45.00
Ituri 8_10	/	A9-029-P-0956-0962	Riv. Bango in Bango, tributary of the Ituri	48.60
Ituri 8_11	/	A9-029-P-0956-0962	Riv. Bango in Bango, tributary of the Ituri	48.85
Ituri 8_12	3347	A9-29	Riv. Bango in Bango, upstream of the bridge along the mining operation, bassin Ituri	45.70

B

Species	Label	Collection	Location	SL (mm)
*E. miolepis*_1	holotype		Riv. Yembe in Banzyville (Ubangi river system)	63.9
*E. holotaenia*_1	syntype	1882.2.13.7	Riv. Ogowe in Gaboon	65.40
*E. holotaenia*_2	syntype	1888.12.13.31 and 1889.3.2.10	Riv. Ogowe in Gaboon	84.95
*E. holotaenia*_3	syntype	1888.12.13.31 and 1889.3.2.10	Riv. Ogowe in Gaboon	88.50
*E. holotaenia*_4	syntype	1869.5.3.23-24	Riv. Ogowe in Gaboon	58.60
*E. holotaenia*_5	syntype	1869.5.3.23-24	Riv. Ogowe in Gaboon	64.55
*E. holotaenia*_6	syntype	1896.5.5.107.112	Riv. Ogowe in Gaboon	66.90
*E. holotaenia*_7	syntype	1896.5.5.107.112	Riv. Ogowe in Gaboon	79.75
*E. holotaenia*_8	syntype	1896.5.5.107.112	Riv. Ogowe in Gaboon	62.95
*E. holotaenia*_9	syntype	1896.5.5.107.112	Riv. Ogowe in Gaboon	67.50
*E. holotaenia*_10	syntype	1896.5.5.107.112	Riv. Ogowe in Gaboon	66.00
*E. holotaenia*_11	syntype	1898.12.28.8-11	Riv. Ogowe in Gaboon	67.30
*E. holotaenia*_12	syntype	1898.12.28.8-11	Riv. Ogowe in Gaboon	56.00
*E. holotaenia*_13	syntype	1898.12.28.8-11	Riv. Ogowe in Gaboon	64.05
*E. holotaenia*_14	syntype	1898.12.28.8-11	Riv. Ogowe in Gaboon	75.25
*E. holotaenia*_15	syntype	1900.2.17.132	Riv. Ogowe in Gaboon	54.40
*E. eutaenia*_1	lectotype	1864.7.13.52-56	Riv. Huila (Mossamedes) in Angola	70.70
*E. eutaenia*_2	paralectotype	1864.7.13.53-56	Riv. Huila (Mossamedes) in Angola	56.75
*E. eutaenia*_3	paralectotype	1864.7.13.53-56	Riv. Huila (Mossamedes) in Angola	66.35
*E. eutaenia*_4	paralectotype	1864.7.13.53-56	Riv. Huila (Mossamedes) in Angola	67.70
*E. eutaenia*_5	paralectotype	1864.7.13.53-56	Riv. Huila (Mossamedes) in Angola	48.25
*E. eutaenia*_6	paralectotype	1864.7.13.53-56	Riv. Huila (Mossamedes) in Angola	54.80
*E. kerstenii*_1	lectotype	ZMB[1] 6848	Coast opposite to Zanzibar (i.e. probably Bagamayo)	64.31
*E. brazzai*_1	holotype	MNHN[2] 86 404	Riv. Sangha in Mobaka	78.2
*E. tshopoensis*_1	holotype	88-25-P-1587	Kisangani, riv. Tshopo, upstream of the hydroelectric dam, Zaïre	64.35
*E. tshopoensis*_2	paratype	87-42-P-1098	Kisangani, riv. Tshopo, downstream of the hydroelectric dam, Zaïre	74.70
*E. tshopoensis*_3	paratype	88-25-P-1590	Kisangani, riv. Tshopo, downstream of the hydroelectric dam, Zaïre	52.55
*E. tshopoensis*_4	paratype	88-25-P-1591-1592	Kisangani, riv. Tshopo, downstream of the hydroelectric dam, Zaïre	68.95
*E. tshopoensis*_5	paratype	88-25-P-1594-1595	Kisangani, riv. Tshopo, downstream of the hydroelectric dam, Zaïre	53.20
*E. tshopoensis*_6	paratype	88-25-P-1605	Kisangani, riv. Tshopo, downstream of the hydroelectric dam, Zaïre	48.75

*E. pellegrini*_1	lectotype	MNHN 35 80	Lake Kivu	52.90
*E. pellegrini*_2	paralectotype	MNHN 35 81	Lake Kivu	37.95
*E. pellegrini*_3	paralectotype	MNHN 35 82	Lake Kivu	36.15
*E. pellegrini*_4	paralectotype	MNHN 1996 265	Lake Kivu	43.25
*E. atromaculatus*_1	paratype	AMNH[3] 5845	Riv. Yakuluku, Lower Congo	41.14
*E. atromaculatus*_2	paratype	AMNH 6214	Riv. Yakuluku, Lower Congo	40.65

[1] Museum für Naturkunde, Berlin, Germany.

[2] Muséum national d'Histoire naturelle, Paris, France.

[3] American Museum of Natural History, New York, USA.

Appendix 2. PC loadings of the PCA in Fig. 3. Most important loadings indicated in bold.

	PC1	PC2	PC3
LogSL	0.229	0.158	-0.033
LogHL	0.236	0.018	-0.037
LogED	**0.271**	**-0.626**	**-0.661**
LogSnL	**0.279**	-0.060	0.230
LogPrOpD	0.244	-0.062	-0.003
LogIOW	0.232	0.163	-0.091
LogPrDD	0.229	0.210	-0.148
LogPoDD	0.238	0.289	0.068
LogDoFBL	0.242	-0.310	**0.395**
LogDoFL	0.216	**-0.310**	**0.528**
LogPrPecD	0.224	0.030	-0.005
LogPrPelD	0.233	0.074	-0.011
LogPrAD	0.236	0.061	-0.096
LogPoAD	0.223	**0.460**	-0.160
LogBD	**0.275**	0.060	0.005
LogMxCPD	0.260	-0.057	0.045
LogMnCPD	0.247	0.024	0.043

Appendix 3. PC loadings of the PCA in Fig. 4. Most important loadings indicated in bold.

	PC1	PC2	PC3
LL Sc	0.242	**0.538**	0.195
D-L Sc	**0.440**	-0.005	-0.196
PD Sc	0.311	**0.376**	-0.047
CP Sc	0.288	0.327	-0.043
LP Sc	**0.371**	-0.339	0.376
L-B Sc	**0.441**	-0.213	**0.397**
DFR	-0.258	-0.285	0.213
AFR	-0.056	0.090	**-0.513**
PecFR	-0.248	0.312	0.224
PelFR	-0.325	**0.341**	**0.513**

Appendix 4. PC loadings of the PCA in Fig. 5. Most important loadings indicated in bold.

	PC1	PC2	PC3
LL Sc	**0.940**	-0.040	-0.023
D-L Sc	0.139	-0.097	-0.084
PD Sc	0.136	**-0.226**	**0.855**
CP Sc	**0.192**	-0.150	**-0.410**
LP Sc	0.044	-0.033	-0.030
L-B Sc	0.140	-0.174	-0.117
DFR	<0.001	<0.001	<-0.001
AFR	0.029	**0.238**	**0.279**
PecFR	**0.142**	**0.910**	0.039
PelFR	0.000	0.000	0.000

Appendix 5. PC loadings of the PCA in Fig. 6. Most important loadings indicated in bold.

	PC1	PC2	PC3
LLSc	**0.480**	0.251	-0.120
D-LSc	0.395	0.189	0.404
PDSc	**0.416**	0.226	**-0.519**
CPSc	**0.512**	0.003	-0.020
L-BSc	0.317	**-0.283**	**0.604**
DFR	0.221	**-0.584**	0.005
AFR	0.071	0.274	-0.040
PecFR	-0.154	**0.595**	**0.430**

Appendix 6. PC loadings of the PCA in Fig. 7. Most important loadings indicated in bold.

	PC1	PC2	PC3
LL Sc	**0.740**	-0.164	0.202
D-L Sc	<-0.001	<-0.001	<-0.001
PD Sc	-0.011	-0.097	**0.402**
CP Sc	-0.105	**0.552**	**0.767**
LP Sc	0.099	-0.403	0.208
L-B Sc	0.132	**-0.501**	0.284
DFR	0.031	-0.054	-0.034
AFR	-0.071	0.050	0.007
PecFR	**0.457**	**0.455**	**-0.290**
PelFR	**0.447**	0.182	0.026

Appendix 7. PC loadings of the PCA in Fig. 8. Most important loadings indicated in bold.

	PC1	PC2	PC3
LL Sc	**0.971**	-0.119	-0.142
D-L Sc	**0.144**	**0.223**	-0.096
PD Sc	0.052	0.219	**-0.187**
CP Sc	0.028	**0.902**	**-0.222**
LP Sc	<-0.001	<-0.001	<0.001
L-B Sc	-0.015	0.053	-0.050
DFR	<-0.001	<0.001	<-0.001
AFR	<-0.001	<-0.001	<0.001
PecFR	**0.179**	**0.267**	**0.928**
PelFR	0.006	0.001	0.152

Appendix 8. PC loadings of the PCA in Fig. 9. Most important loadings indicated in bold.

	PC1	PC2	PC3
LL Sc	**0.971**	-0.073	-0.141
D-L Sc	**0.175**	0.047	**0.144**
PD Sc	0.051	**-0.322**	-0.092
CP Sc	**0.118**	-0.085	**0.953**
LP Sc	<0.001	<0.001	<-0.001
L-B Sc	<-0.001	<-0.001	<0.001
DFR	<-0.001	<-0.001	<0.001
AFR	0.000	0.000	0.000
PecFR	0.092	**0.904**	0.090
PelFR	0.024	**0.254**	**-0.185**